JOURNAL OF MATERIALS SCIENCE **35** (2000) 4231–4242

Super-plastic behavior of the brittle polymer film in multilayer systems

C. H. LIN, A. C.-M. YANG
Department of Material Science and Engineering, National Tsing Hua University, Hsinchu, Taiwan
E-mail: AcyAng@MSE.Nthu.edu.TW

Crazes are usually observed preceding brittle fracture of glassy polymers. They were believed to result from a necking process similar to that in fiber drawing. In this study, we further exploited the necking characteristic of crazing by sandwiching the craze-forming brittle polymer film between two ductile polymer films to examine the deformation behavior of the brittle polymer when necking is suppressed. We found that when necking was suppressed, the brittle polymer film demonstrated a super-plastic behavior in that the film could be stretched to a very large deformation without any strain localization or cracking, and this deformation was shown to be mostly plastic. The super-plastic behavior is remarkably dependent on the thickness of the outer ductile polymer layers. When the outer-layer thickness is less than a critical thickness, the brittle polymer film in combination with the sandwich structure demonstrated a different degree of strain localization with the critical strain increased with the thickness of the outer-layer. The microstructure of deformation zones in the multi-layer samples was investigated by atomic force microscopy (AFM). The effect of the interfacial strength at the polymer interfaces was also investigated by SIMS and discussed.

1. Introduction

Under an external force, a glassy polymer first deforms elastically and uniformly and then yields when the applied stress is greater than the yielding stress [1]. When glassy polymer yields, the deformation is usually localized into some weak points and subsequently induces brittle fracture. The strain localization of the glassy polymer in the brittle polymers is usually in the form of crazes [2–4], which unlike cracks are load-bearing areas because their two surfaces are bridged by many microfibrils with mean diameter of a few nanometers [5]. Due to the highly concentrated stress, these microfibrils are susceptible to breakdown which will subsequently trigger crack propagation [3, 6, 7]. The extension ratio of the crazed region had been measured by Kramer using a TEM micro-densitometry technique [8, 9]. For polystyrene, the craze extension ratio was found to be around 400%, far more than the fracture strain of the tested sample. The remarkably large extension ratio in the crazes suggests that under certain conditions glassy polymer can be stretched to a very large strain without fracture.

The mass density distribution across a craze, extracted from craze TEM micrographs, suggests a surface drawing mechanism operative during crazing [10–12]. That is, during crazing, there is an active zone at the interface of the craze and matrix from which a growing craze draws new material into the crazed region. Further, from the data taken from the experiments using atomic force microscope (AFM), it was also found that a craze actually is a highly depressed region with its depth increasing with craze width until it finally saturates when a critical width is reached [13]. This strongly suggests that a micro-necking process is also operative during crazing in a way very similar to that of polymer yielding either of a macroscopic or microscopic scale [1, 14–16]. It would be very interesting to explore the deformation behavior of a brittle polymer, e.g., polystyrene, when the micro-necking process is suppressed. In this paper, we used a multi-layer sandwiching technique to suppress the micro-necking.

In the past, similar sandwiching technique had been used to improve polymer fracture toughness although the focus of research was not centered on the role of micro-necking during crazing. Baer *et al.* [17–22] used a multi-layer polymer co-extrusion process to prepare multi-layer films consisting of a hundred alternating layers of SAN and PC. They found that increasing the number of alternating layers of the films will lead to an increase of fracture toughness and at the same time the fracture mode in the brittle SAN layers transforms from crazing to the formation of a shear deformation zone. Umemoto *et al.* [23, 24] also studied the toughening effect in laminated PE/PS/PE sandwiched structure. It was found that the crazing stress of PS was dependent on the volume fraction of PE in the sandwich and this effect was attributed to the reduction of the tensile stress concentration at the craze tip. In our system of PPO/PS/PPO multi-layer structure, if the crazing process is suppressed due to the constraining effect of the

outer layers, the fracture toughness should be extraordinarily improved. Hence, our result can provide a new direction for toughening glassy polymers.

2. Experiments

The polymers used in the multi-layer structures are polystyrene (PS) and Poly(2,6-dimethyl-1,4-phenyl oxide) (PPO). The PPO was purchased from the Aldrich Chemical Company. It has a molecular weight of $M_w = 244{,}000$ and $M_n = 32{,}000$. The PS was purchased from the Pressure Chemical Company, with $M_w = 2{,}000{,}000$ and $M_w/M_n = 1.3$. The polymer was fully dissolved in toluene before thin film casting. To assist its dissolution, heating to a moderate temperature around 100°C before casting was required. The thickness of PS films was either 0.1 μm or 0.07 μm. For PPO films, various thicknesses were prepared: 0.1 μm, 0.2 μm 0.3 μm, 0.4 μm, 0.5 μm, and 0.6 μm. When the cast film of the polymer was completely dried on the glass slide substrate, it was transferred to the copper grids by first floating off to a water surface and then picked up by a piece of copper grid. The films on the copper grid were dried in air at room temperature for at least a day. For making the multi-layers, the dried thin film on the copper grids was used to pick up the next polymer layer from the water surface following a similar procedure. Each piece of copper grid had at least 20–30 separate squares, and the film area perfectly bonded on each square and can be regarded as an independent specimen. The multi-layer structure is illustrated as Fig. 1. Before mechanical testing and examination, the polymer films were treated in toluene vapor briefly to enhance the adhesion between polymer thin film and the copper grids. After the toluene vapor treatment, the samples were stored at the ambient conditions for at least 12 hrs to make sure no toluene left in the polymer.

The multi-layer system was then manually stretched by a strain jig, and the strain rate was controlled as slow as possible to be in the range of 10^{-4}–10^{-5}/s to prevent the adiabatic heating effect due to deformation [25, 26]. During the straining process, the sample was observed by using an optical microscope to measure the critical strain for initiation of the local deformation zones, which was defined as more than half of the grid squares had undergone deformation zone initiation. The morphology of the growing deformation zones was also investigated. To calculate the degree of strain localization of the multilayer system, the width of crazes had been measured directly by LECO 2000 digital image analysis system under 500 magnification. Further, the deformation zones were scanned by an AFM (Digital Instrumental, Nanoscope IIIa) to explore the topography and interior microstructure of the strained regions. For the purpose of comparison, an incompatible multilayer system of polycarbonate (PC)/PS/ polycarbonate (PC) was prepared. The PC was acquired from PolyScience. The solvent used for PC was chloroform and the thickness of the multi-layer systems were 0.8 μm PC/ 0.6 μm PS/0.8 μm PC and 0.08 μm PC/0.6 μm PS/ 0.08 μm PC.

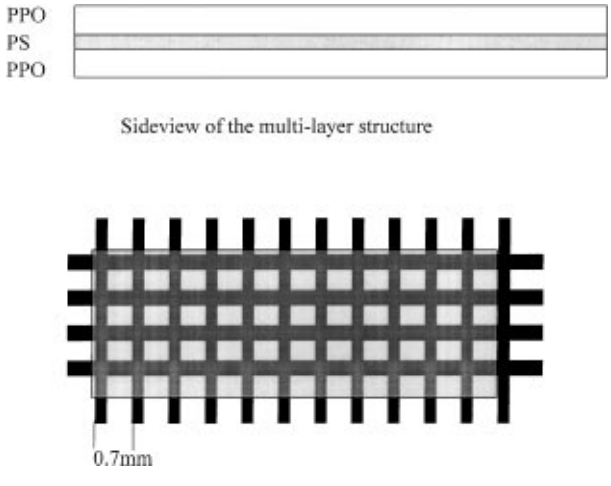

Figure 1 A schematic drawing of the multi-layer structure.

3. Results and discussions

3.1. The super-plastic behavior of the multilayer films

The micrograph of the single layer 0.1 μm PS film at 10% strain is illustrated as in Fig. 2. It is worth noticing that nearly all the crazes in PS thin film propagate across the whole specimen. Fig. 3 shows that the accumulative fraction of the crazed specimens increases with the applied external strain and the critical strain is around 0.9%, independent on the film thickness. This observation is very similar to that reported elsewhere before [27].

PPO is known as a good engineering polymer with superior mechanical properties and good miscibility with PS. The fresh single layer PPO films (ca. 0.5 μm thick) could be uniformly deformed up to more than 25% when the grid bars of the copper grid broke without the formation of any local deformation zones. However, when PPO films aged even in the ambient conditions for 1 week, embrittlement effects appeared in that local deformation zones initiated during deformation and the sample broke at relatively low strain [28]. Therefore, all PPO films were used and tested within one week after preparation.

It is desirable to quantitatively describe the degree of the strain localization in polymer films, a new parameter ζ was defined as the fraction of the actual total width of local deformation zones along the strained direction to the total sample length increase from deformation. If no strain localization was observed, $\zeta = 0$. On the other hand, $\zeta = 100\%$ means that the entire applied deformation concentrates in the local deformation zone, and the matrix outside sustains no deformation. The relationship between the ζ of PS craze and the applied strain is shown as Fig. 4. It demonstrates that when crazing initiated, nearly all the strain incurred concentrated into the crazed area.

The topography of a craze obtained from AFM scanning is shown in Fig. 5. It can be seen that a craze is a conspicuously depressed region. The depth of the craze as a function of craze width is shown in Fig. 6. Initially the depth of depression increases linearly with craze

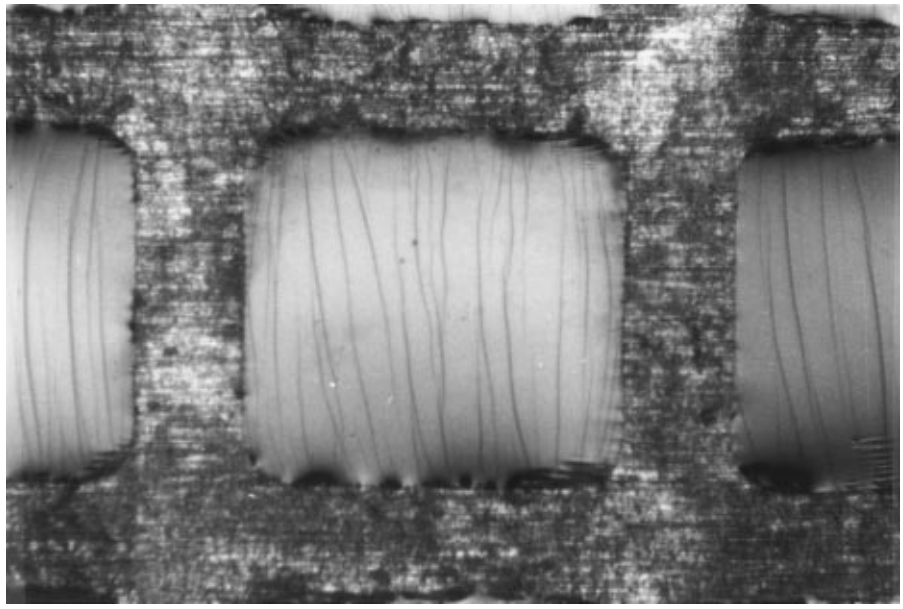

Figure 2 An optical micrograph of a craze in a 0.1 μm PS film at 10% strain ($\times$65).

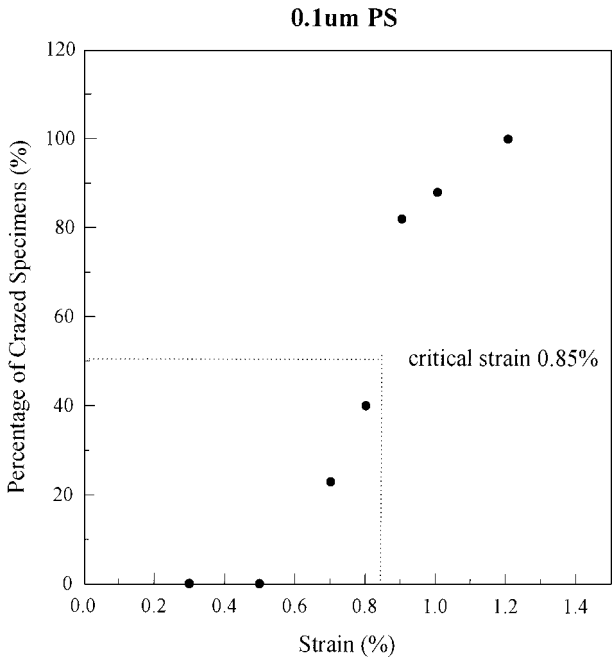

Figure 3 The accumulated percentage of crazed units in a specimen versus the applied strain.

TABLE I The topographic data of the deformation zones in the PPO/PS/PPO multi-layers

	Depth of plateau	Slope of incline	Critical width
0.1 μm PS	60 nm	0.06	1000 nm
0.07 μmPPO/0.1 μm PS/0.07 μmPPO	80 nm	0.04	2000 nm
0.1 μmPPO/0.1 μm PS/0.1 μmPPO	90 nm	0.02	4500 nm
0.2 μmPPO/0.1 μm PS/0.2 μmPPO	100 nm	0.16	6000 nm

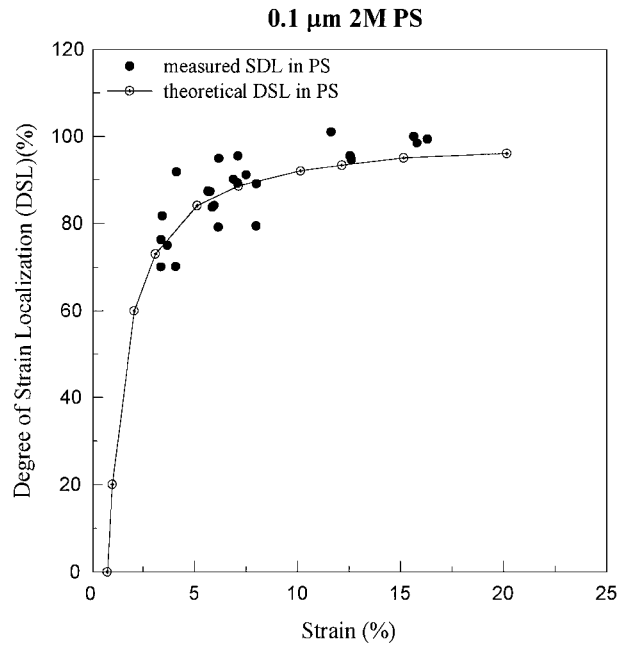

Figure 4 The relationship between the degree of strain localization ζ and the applied strain in 0.1 μm PS films.

width until a maximum depth is reached. When craze width is equal to a critical value, then the depth levels off. The drawing process of crazing therefore is very similar to a necking process that operates in a microscopic scale [20]. For a 0.1 μm thick PS film, the critical width is about 1000 nm, the depth of plateau is 60 nm, and the slope at the neck shoulder, the socalled active zone, is 0.06, as shown in Table I.

Since the formation of craze and the triggering of brittle fracture of glassy polymers is resulted from a micro-necking process, when necking is restricted the polymer films may be deformed uniformly for as long as the restriction of necking is effective. To restrict the micro-necking, a multi-layer structure composed of a craze-forming PS film sandwiched between two ductile PPO films was prepared. The surface depression occurring during a micro-necking process in PS film would be constrained by the adhesion of the PS film to the outer PPO films that deform uniformly. Fig. 7 shows a 0.62 μm PPO/0.1 μm PS/0.62 μm PPO sample

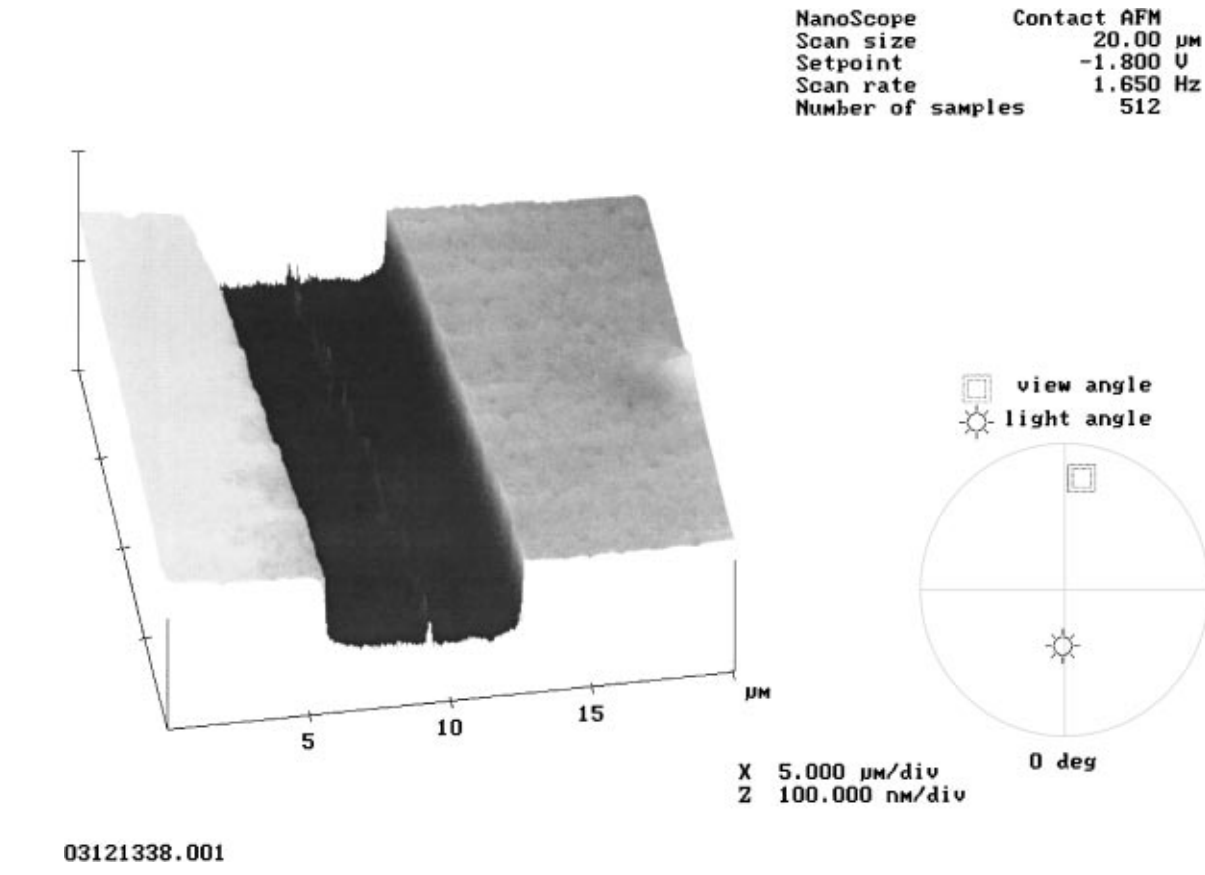

Figure 5 The AFM photography of a 0.1 μm PS craze.

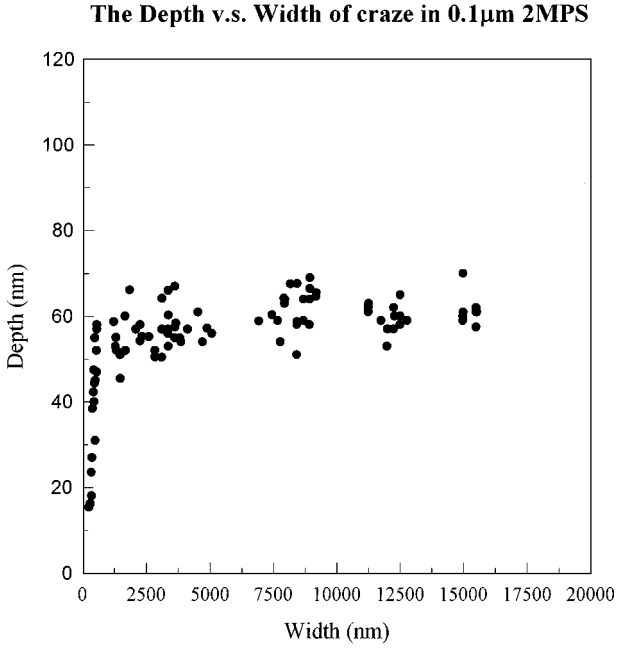

Figure 6 The relationship of depth and craze width of crazes in 0.1 μm PS thin film.

demonstrating impressive uniform deformation behavior up to a 10% strain. The copper grids used to break at roughly 25% strain, therefore it is impossible to test the multi-layer sample beyond that strain limit. The same behavior was also observed in the 0.5 μm PPO/0.1 μm PS/0.5 μm PPO sample. The outstanding mechanical property of the brittle polymer in a multilayer structure demonstrates that if the micronecking mechanism can be suppressed, then the craze as well as the strain localization can be "switched off". This in turn unambiguously shows that micro-necking is necessary for crazing. Furthermore, it is obvious that multi-layering is an effective approach to toughen brittle polymers in that it can restrict the formation of crazes. The large deformation in the above multi-layer samples was demonstrated to be mostly, if not entirely, plastic as the sample dimension measured after the applied load was removed indicated only a small shrinkage of 2.5%, the elastic component of the ca. 25% strain, very close to the crazing strain (ca. 1%) of the brittle PS film.

For the single PS layer the crazed region was usually under 5% of the whole specimen area. However for the multilayer structure, then the super-plastic behavior allowed uniform deformation without strain localization, then the total toughness will be at least 20 times that of the single layered PS. The toughness can be much more improved in multilayer structure than in single PS because of the uniform deformation.

3.2. The effects of the thickness of the constraining layers

The super-plastic behavior of the multilayer system, however, is remarkably dependent on the PPO thickness. This thickness effect is not difficult to rationalize as thicker PPO layer should have a higher buckling stress to resist the local necking stress in the PS film. Fig. 8a, b, and c show that when the PS film thickness was kept constant at 0.1 μm, the sandwiched samples with PPO films thinner than 0.3 μm, e.g.,

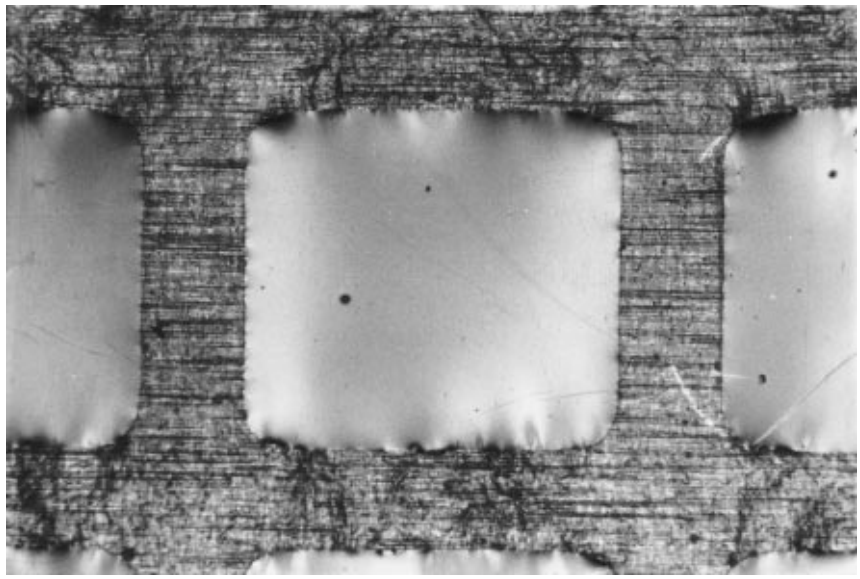

Figure 7 The optical micrograph of a highly strained (10% strain) multi-layer structure of 0.6 μm PPO/0.1 μm PS/ 0.6 μm PPO ($\times$65).

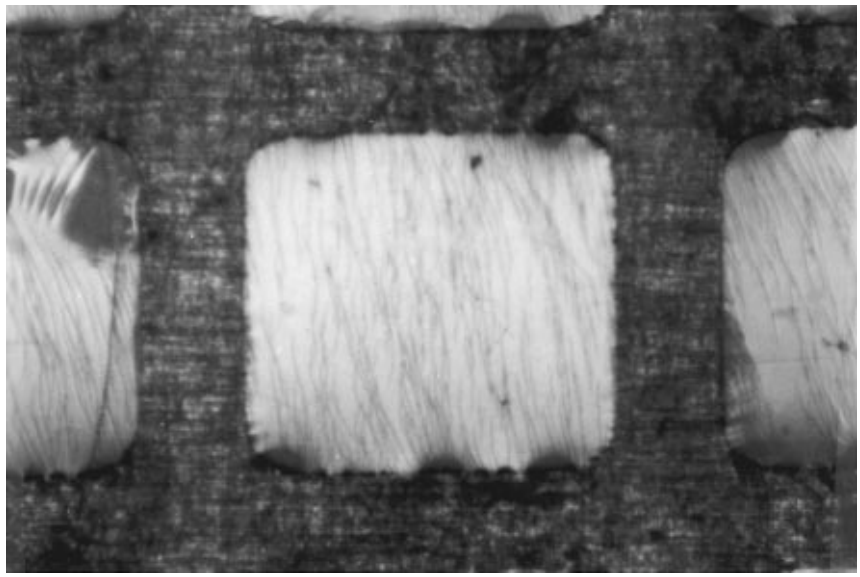

(a)

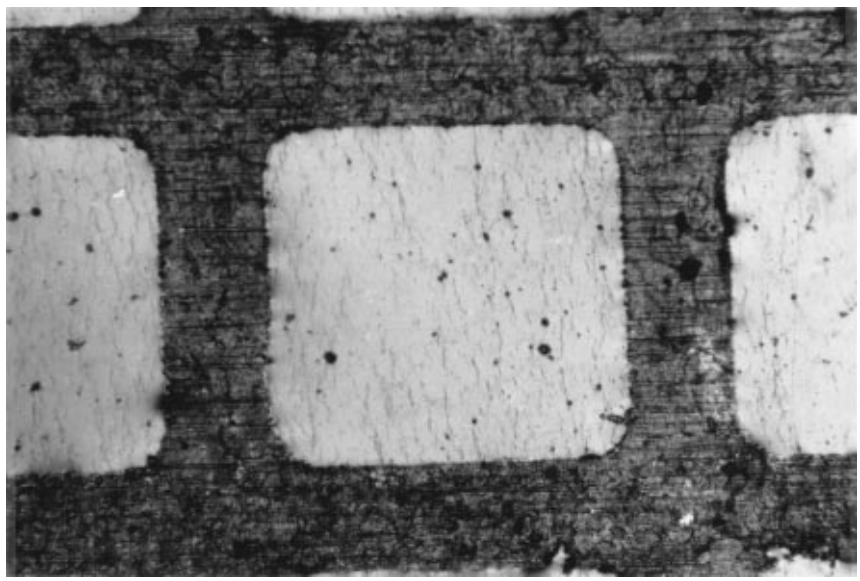

(b)

Figure 8 The optical micrograph of strained multi-layer structure of (a) 0.07 μm PPO/0.1 μm PS/0.07 μm PPO at 10% strain (b) 0.1 μm PPO/0.1 μm PS/0.1 μm PPO at 5% strain (c) 0.2 μm PPO/0.1 μm PS/0.2 μm PPO at 5% strain ($\times$65). (*Continued*)

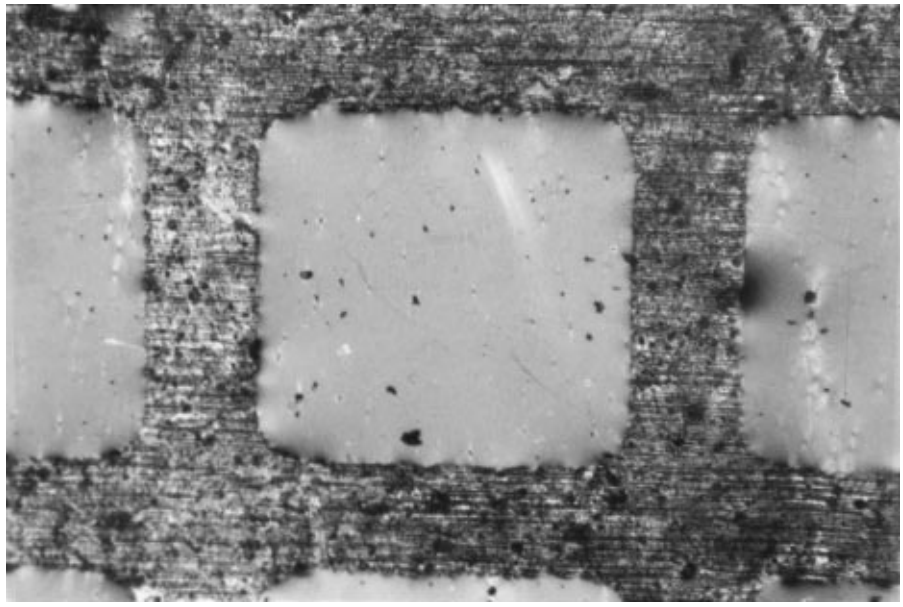

(c)

Figure 8 (*Continued*).

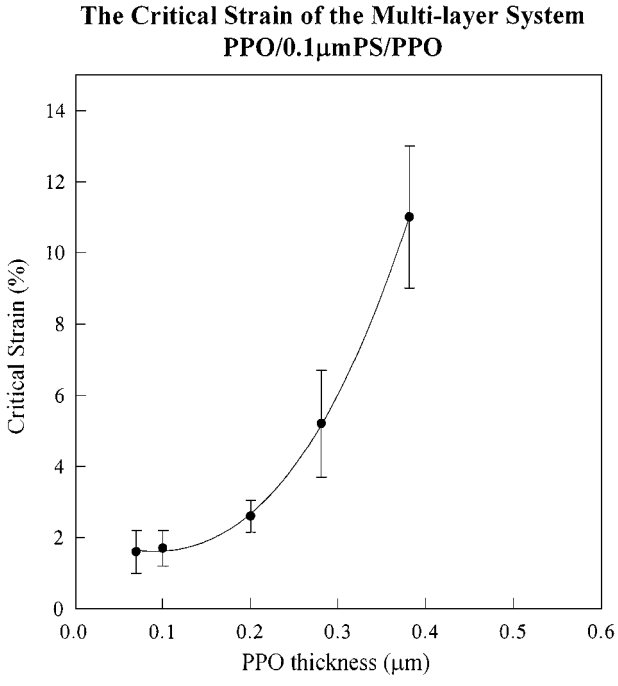

Figure 9 The critical strain of crazing of the multi-layer structure with various PPO thickness.

0.07 μm/0.1 μm/0.07 μm, 0.1 μm/0.1 μm/0.1 μm, and 0.2 μm/0.1 μm/0.2 μm, showed extensive strain localization. The critical strains of these multi-layer systems are given in Fig. 9. It can be seen that all the critical strains of these multi-layer structure are larger than that of the PS crazing stain, and the critical strain increases with PPO thickness. For those systems with PPO thickness less than 0.3 μm, the critical strain is around the crazing strain of PS, and this result reflected the failure of constraint of the outer PPO film in preventing the nucleation of the strain localization. However, if the thickness of PPO film is larger than 0.3 μm, not only the critical strain increases rapidly but the morphology of the deformation zone also changes as Fig. 10 shows. Meanwhile, the initiation of the local deformation zones is ambiguous and difficult to define precisely in those systems. This ambiguity results in the extensive variation of the critical strain. The delay of the strain localization in multi-layer structures can stem from the inhibition of the micro-necking mechanism by the constraint of the outer PPO films. If the thickness of PPO film is enough that the micro-necking mechanism can be switched off, then the formation of the craze as well as the strain localization, of the brittle polymer film can be depressed, therefore the super-plasticity can occur, as shown in Figs 7 and 10.

The degree of strain localization (ζ) values of the multi-layer systems with PPO thickness less than 0.3 μm are shown in Fig. 11. In a sharp contrast to that of the single layer PS films in which ζ saturated at as little as 5% strain in single PS film, there is no obvious saturation even at large strains over 20%. In single PS film the strain localized into the crazed region as soon as crazes initiated and the un-crazed region sustained only a small elastic strain (ca. 0.9%). The ζ in the multi-layer structure increased slowly with the applied strain and even at large strain the ζ was still much less than 100%. The very small ζ in the multi-layer systems indicates that even in the cases where the local deformation zones occur, the matrix can still sustain a significant degree of deformation. The delay of the critical strain and the decline of the degree of strain localization, manifest even when the PPO thickness is not enough, the toughness of the multi-layer, or the trend to strain localization, can be modified by the multi-layer structure.

3.3. The morphology and microstructure of the local deformation zones

The morphology of the deformation zones in the multi-layer samples was evidently different from the crazes in the single layer PS films. They ceased to propagate at a much shorter length than those in the single layer PS

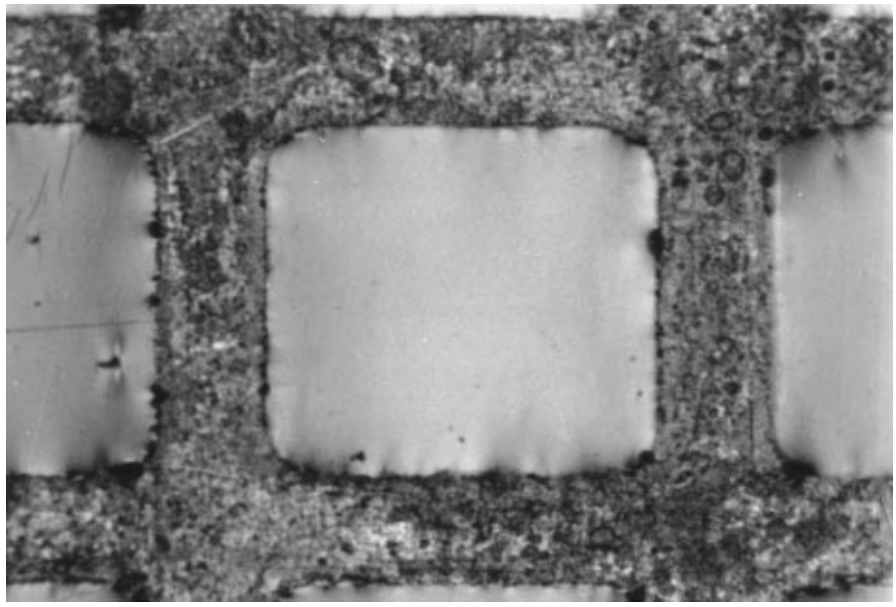

(a)

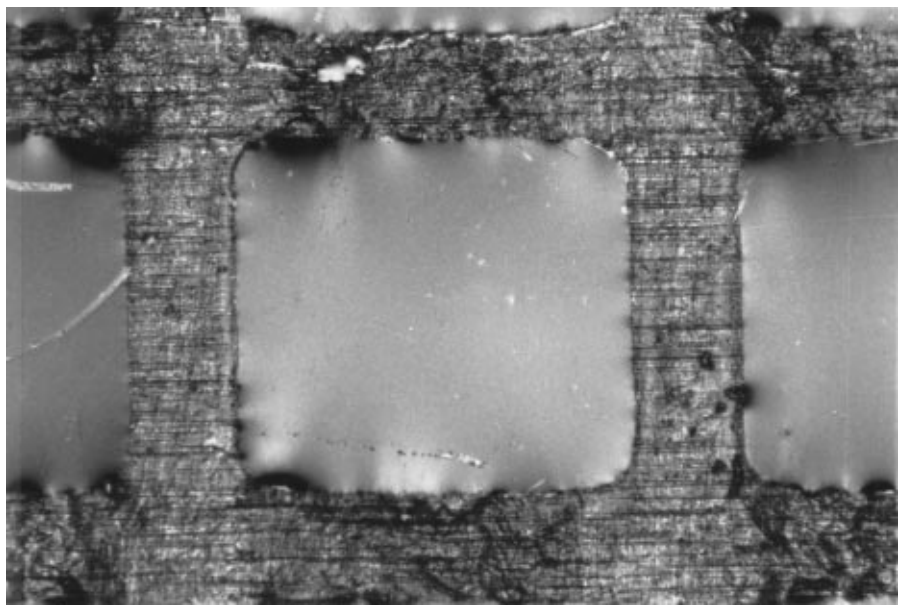

(b)

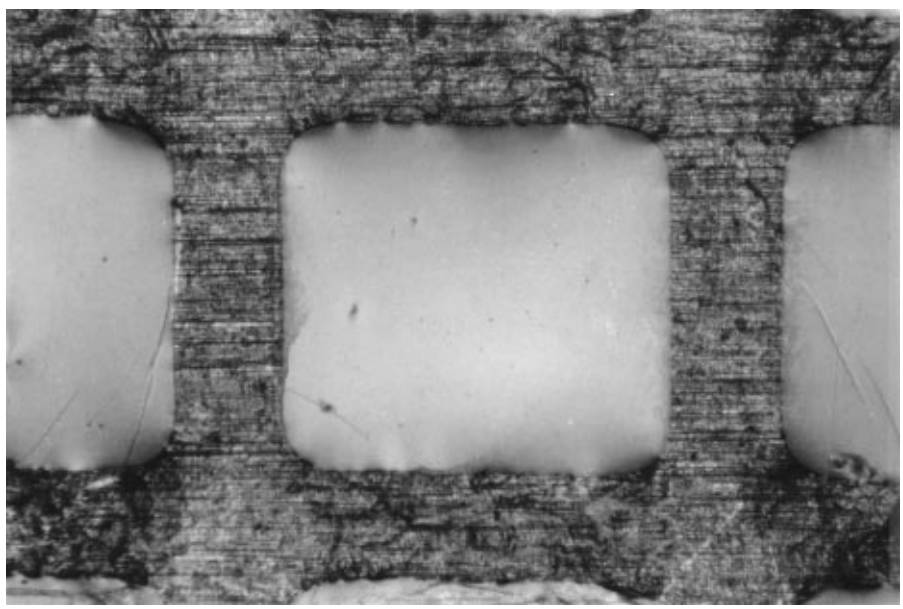

(c)

Figure 10 The optical micrograph of strained multi-layer structure of (a) 0.3 μm PPO/0.1 μm PS/0.3 μm PPO at 10% strain. (b) 0.4 μm PPO/0.1 μm PS/0.4 μm PPO at 10% strain. (c) 0.5 μm PPO/0.1 μm PS/0.5 μm PPO at 10% strain ($\times$65).

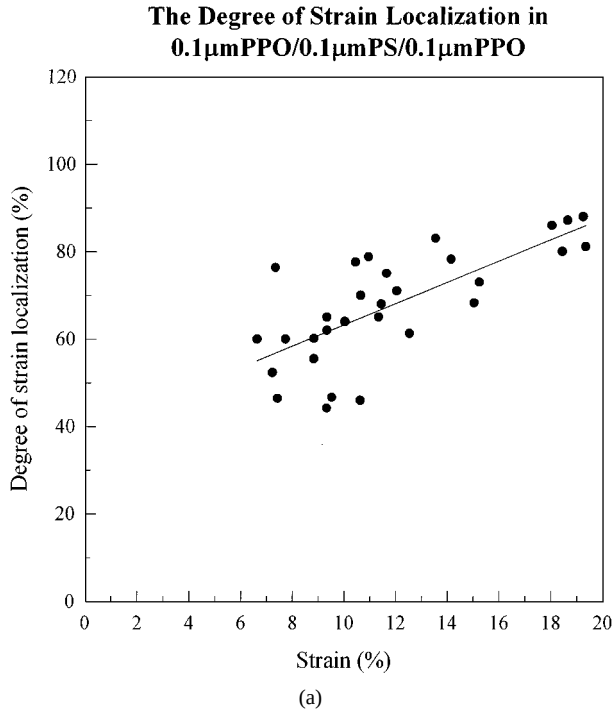

(a)

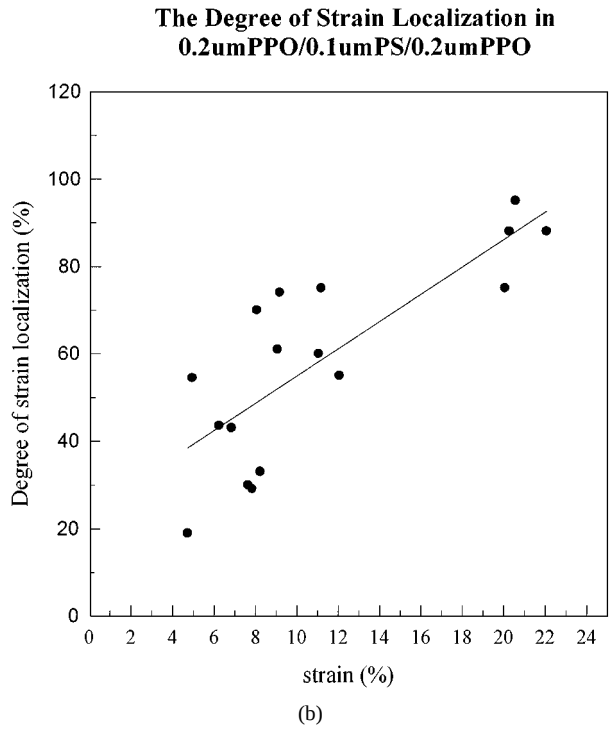

(b)

Figure 11 The degree of the strain localization ζ in the multi-layer structures at different strain: (a) 0.1 μm PPO/0.1 μm PS/0.1 μm PPO (b) 0.2 μm PPO/0.1 μm PS/0.2 μm PPO.

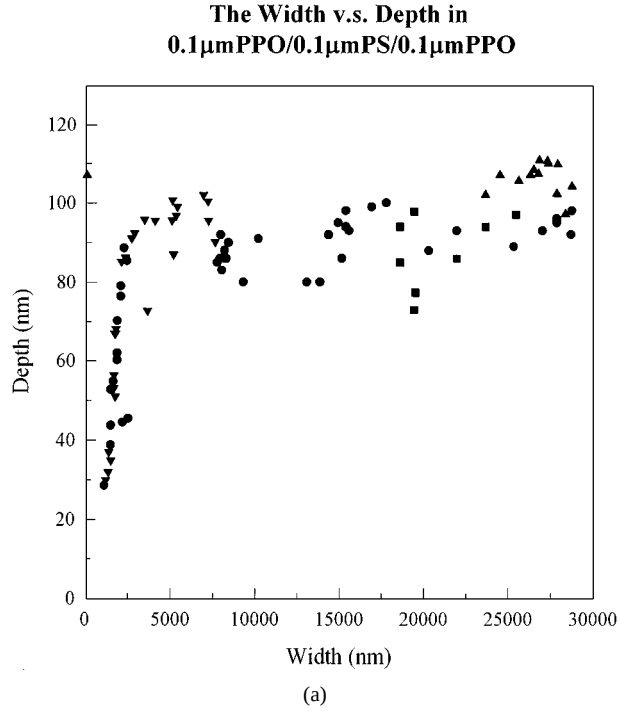

(a)

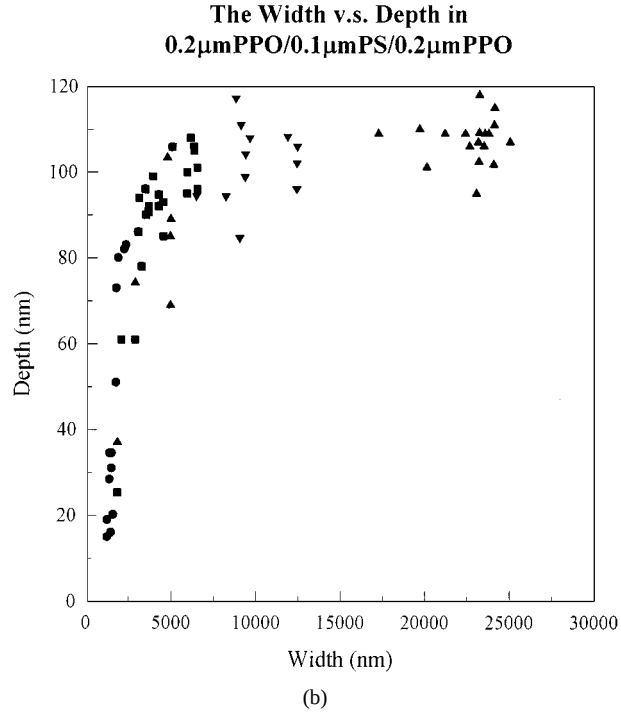

(b)

Figure 12 The depth versus the craze width of the local deformation zones in the multi-layer structure: (a) 0.1 μm PPO/0.1 μm PS/0.1 μm PPO (b) 0.2 μm PPO/0.1 μm PS/0.2 μm PPO.

films, where almost all the crazes ran across the whole specimen (Fig. 2), indicating that the growth of these deformation zones has indeed been constrained by the multi-layer structure. For the multi-layer samples with thicker PPO layers (thicker than 0.3 μm), the deformation zones are hard to define and very different from that previously discussed. If the outer PPO thickness is more than 0.3 μm, the constraint of the multi-layer structure is effective.

The depth of the local deformation zones, obtained from AFM scanning, versus zone width are shown in Fig. 12 for various PPO thickness. The topographic data of the local deformation zones in the multilayer systems is illustrated in Table I. It can be seen that the critical width of the deformation zone in these multilayer systems increased linearly with PPO thickness, as shown in Fig. 13. The same trend of the depth of the plateau is also shown in Fig. 14. The increase of both the critical width and the plateau depth with the PPO thickness indicates that the growth of deformation zones in the multi-layers was retarded, and when the PPO thickness became more than 0.3 μm, the strain localization completely vanished. The retardation of the growth, and therefore the breakdown, of the deformation zones

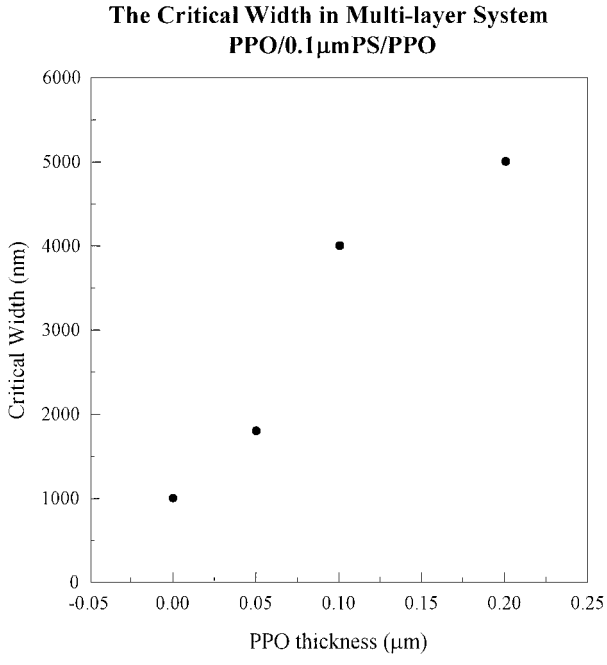

Figure 13 The critical with of local deformation of the multi-layer structure with different PPO thickness.

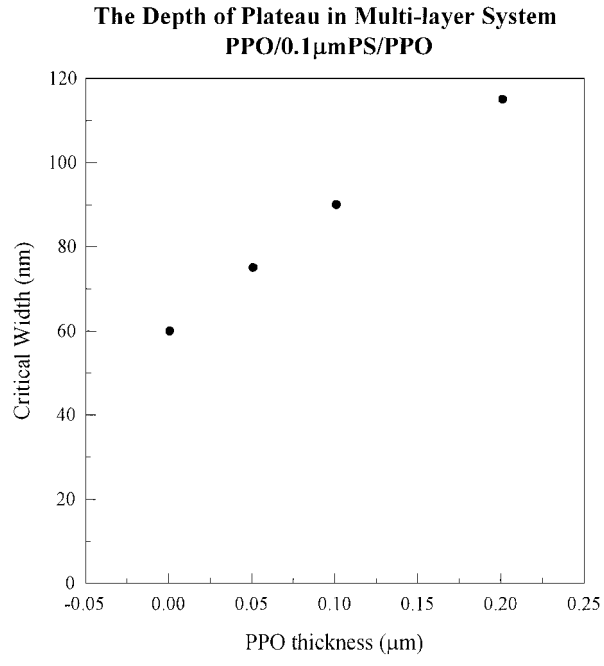

Figure 14 The plateau depth of the deformation zones in multi-layer structure with different PPO thickness.

greatly increases the toughness of the brittle polymer film because more energy is needed to generate a mature deformation zone.

Furthermore, the formation of the local deformation zones in these systems clearly involved the shear deformation of the PPO films as the depth of the deformation zone (ca. 0.12 μm at maturation) is significantly greater than the total thickness of the PS layer.

3.4. The interfacial composition in the multilayer structure

Due to the good miscibility between PPO and PS, polymer chain interdiffusion may occur and result in local blending of PPO and PS near the interfaces. If the local blending of the PS and PPO chains became extensive, the mechanical properties of the brittle PS film sandwiched between the PPO layers undoubtedly will change to a ductile behavior, making the effect of micronecking suppression indistinguishable. To clarify this confusion, we analyzed the composition in the multilayer structure by secondary ion mass spectrometry (SIMS). In the PPO/PS/PPO multi-layers, the oxygen concentration profile across the thickness was used as a marker for probing the interdiffusion of the PPO and PS. Fig. 15 shows the oxygen distribution in the multilayer indicating that there was no extensive interdiffusion of PS and PPO chains. The SIMS results have removed the ambiguity that the observed super-plasticity in the multi-layers was effected from blending of PPO and PS chains.

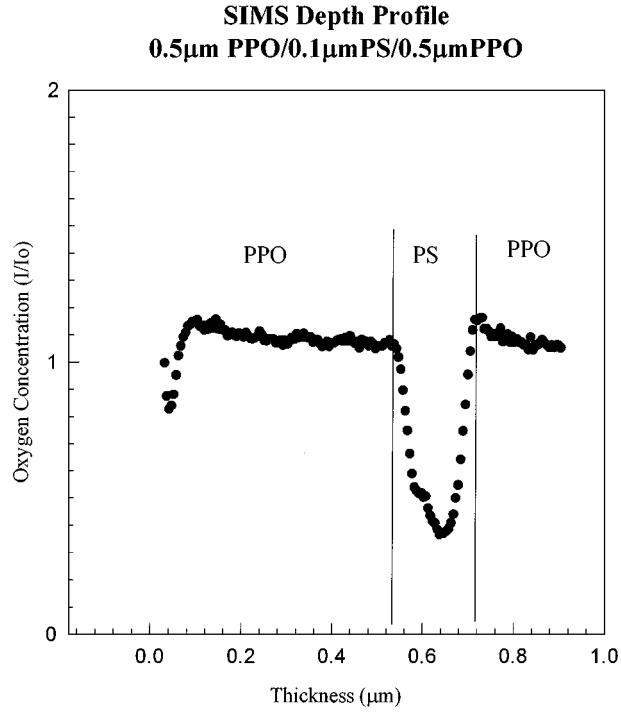

Figure 15 The PPO concentration profile in the thickness direction in a 0.5 μm PPO/0.1 μm PS/0.5 μm PPO multi-layer structure.

Since the super-plasticity is resulted from the constraint of the PPO layers, it is very important that the interfacial strength should be large enough to transfer the load between the PS and PPO layers. If the interfacial strength is too weak, the multilayer may debond. If the interface cannot transfer the necking stress to PPO due to debond between layers, then the super-plasticity will not be observed. In a well-prepared multi-layer sample, the good miscibility between PPO and PS always ensures strong interfaces. Nevertheless, when the procedures of the sample preparation were not well followed, samples with poor interfacial adhesion were obtained, which clearly demonstrated debonding during deformation and super-plasticity failed.

The interfacial thickness in the bilayer of PPO and styrenic copolymers has been studied by Paul *et al.* [29]. They utilized neutron reflection to measure the interfacial thickness between the PPO and styrene-acrylonitrile (SAN) copolymers and between PPO and styrene-maleic anhydride (SMA). It was found that the

interfacial thickness varied with the composition of the copolymer, and more the styrene in the copolymers, the thicker the interfacial thickness. Although there are no data of the interfacial thickness of the pure PS and PPO, however, approximately by extrapolation, the interfacial thickness of PPO and 0% AN in SAN, the interfacial thickness of the PPO and PS can be estimated as 1-2 nm as cast and 15–20 nm after annealing. According to this information, the interfacial thickness in our multilayer structure must be between 2–20 nm due to the toluene vapor treatment step increasing the interdiffusion of the PPO and PS. In our parallel studies it was found that the bilayer PPO and PS would interdiffuse and homogenize if aged at high temperature for a long time, and the bilayer structure remained indissoluble under ambient temperature.

It is believed that the interfacial thickness provides the interfacial strength for the multilayer structure and transfers the induced triaxial stress of PS during necking to PPO. There are extensive literatures on the interfacial strength of polymeric film structure, e.g., Kramer *et al.* studied the interfacial toughness by segregating block copolymers to the interface between immiscible homopolymers. It was found that the interfacial toughness depends on the molecular weight M and the areal density of the diblock copolymer to provide sufficient entanglement at the interface. The fracture mechanism of the interface reinforced with block copolymer can be categorized into two transitions [30]. If $M \gg M_e$ for both blocks, where M_e is the entanglement molecular weight of its respective homopolymer, then the fracture at the interface will change from chain scission to crazing. The other transition is from chain pullout of the diblock copolymer at the interface to crazing ($M < M_e$ for one block) if a high enough areal density can be achieved at the interface. In our case, although no diblock copolymer is used because of interdiffusion of the PPO and PS, there is an interfacial layer of mixed PPO and PS between layers as mentioned above. The molecular weighs of the PPO and PS are much larger than the respective entanglement molecular weight, so the interfacial strength can be effective because of the interfacial layer to transfer the load induced by PS to PPO to constrain the micronecking mechanism.

3.5. The PC/PS/PC multilayer samples

Since the prohibition of micronecking is due to the constraint of the outer ductile films, any ductile films that can deform uniformly in the testing conditions can be candidates for the outer layers. We prepared two multilayer systems, 0.8 μm PC/0.6 μm PS/0.8 μm PC and 0.08 μm PC/0.6 μm PS/0.08 μm PC using polycarbonate (PC) films to replace the PPO films. It was found that the 0.8 μm PC/0.6 μm PS/0.8 μm PC sample, in which the PC thickness is greater than the PS thickness, demonstrated super-plastic behavior as shown in Fig. 16. However, for the very thin PC thickness, the 0.08 μm PC/0.6 μm PS/0.08 μm PC sample failed to show super-plasticity, as depicted in Fig. 17. This is consistent with the results of the PPO/PS/PPO systems that the outer ductile films should be thick enough to ensure super-plasticity. The super-plastic system of 0.8 μm PC/0.6 μm PS/0.8 μm PC is also examined by SIMS, and Fig. 18 shows the depth profile of the PC polymer in the multilayer sample. It is evident that clear interfaces exist in the multilayer, indicating that the super-plastic behavior is due to the suppression of the local necking of the brittle PS film.

3.6. The uniform deformation of the glassy polymer

It is very intriguing that a brittle polymer like PS can be deformed uniformly. During the deformation, what happens in the brittle film of the multi-layers when the applied strain equals the crazing strain of the polymers? It in turns brings another question: what is the physical meaning of crazing strain? All this requires further

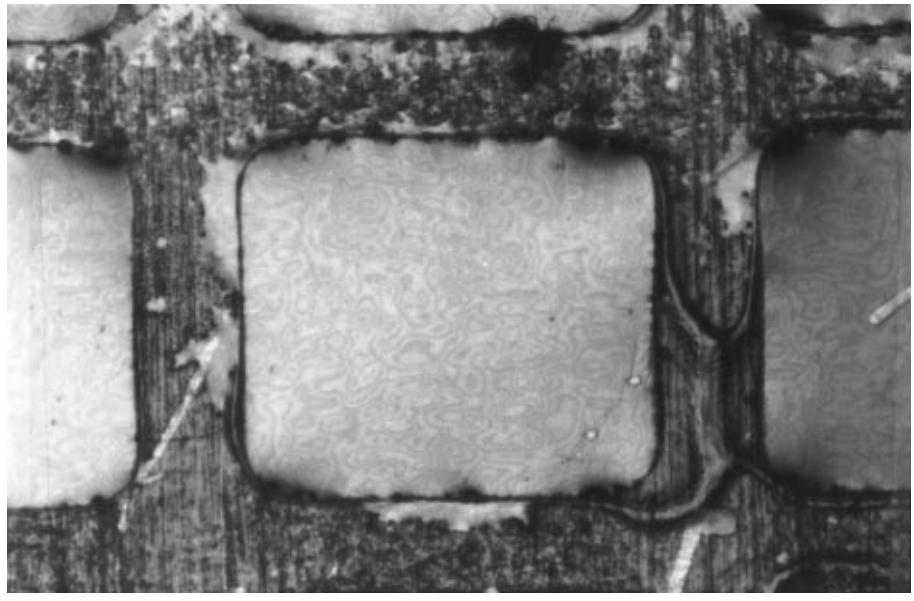

Figure 16 The optical micrograph of the strained multi-layer structure of 0.8 μm PC/0.6 μm PS/0.8 μm PC at 15% strain (×65).

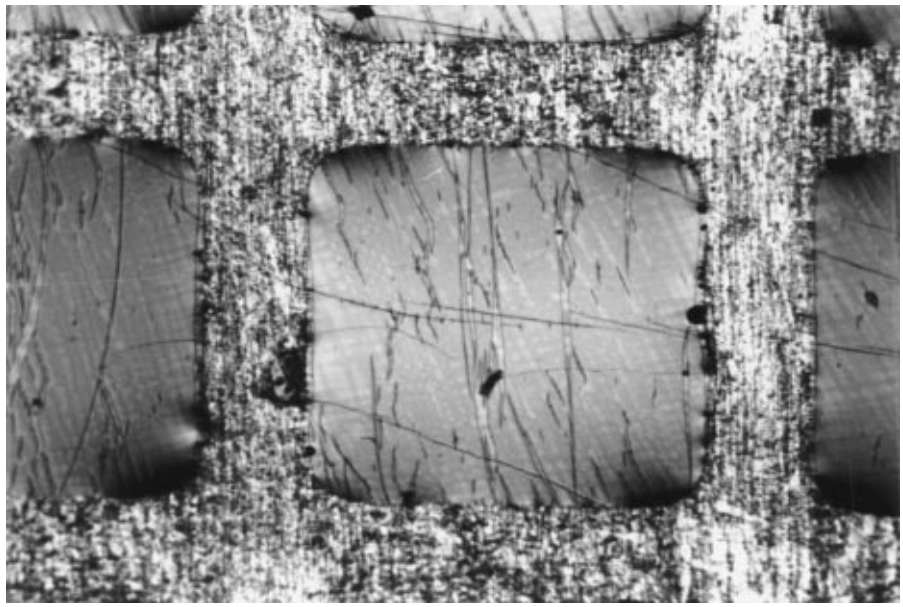

Figure 17 The optical micrograph of the strained multi-layer structure of 0.08 μm PC/0.6 μm PS/0.08 μm PC at 15% strain ($\times$65).

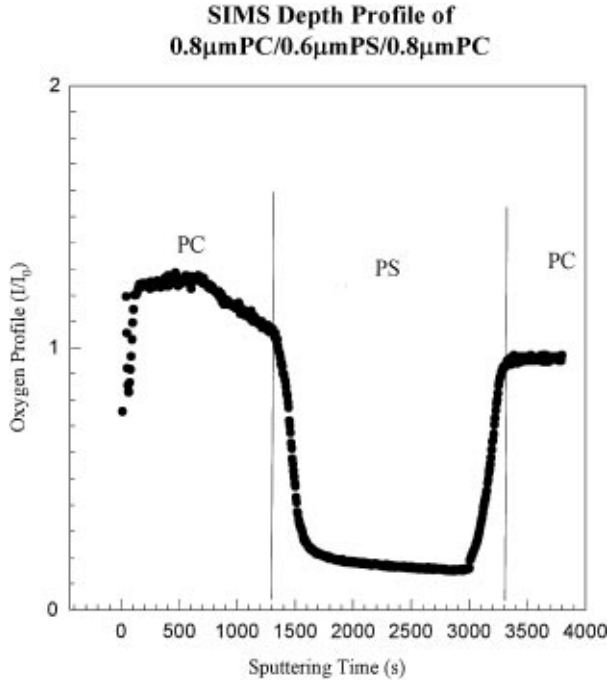

Figure 18 The PPO concentration profile in the thickness direction in a 0.8 μm PC/0.6 μm PS/0.8 μm PC multi-layer structure.

study which should provide very valuable information for us to understand how glassy polymers deform.

4. Conclusions

1. By sandwiching a brittle polymer film between two ductile polymer films, the micronecking mechanism of crazing in the brittle polymer films can be effectively inhibited and the brittle films can be plastically deformed to very large strains without any strain localization.

2. From the topography obtained from AFM data and the super-plastic behavior of the multi-layer structure, it is confirmed that crazing in brittle polymer films is a micro-necking process.

3. By defining the degree of strain localization ζ , it can be shown that crazing is a phenomenon of strain localization, and the degree of strain localization reaches nearly 100% at only 3–4% strain in single PS film.

4. The super-plastic behavior of the multilayer system is dependent on the outer layer thickness. The micro-necking mechanism can be inhibited when the outer layer thickness is greater than a critical value. The same super-plastic behavior is present in both the compatible PPO/PS/PPO and incompatible PC/PS/PC systems.

5. When the outer PPO thickness is not thick enough to stop the strain localization, the deformation zone occurs during extension. However, the critical strain, the critical width of the deformation zone, and the depth of plateau all increase with the PPO thickness. Furthermore, the strain localization in the multi-layer system is greatly reduced with higher PPO thickness.

6. At the sites of the strain localization in multilayer systems, the outer PPO is also depressed and necked, rather than deformed in a conformal behavior.

7. From SIMS data, only very limited polymer diffusion takes place in the PPO/PS/PPO multi-layer systems. The same super-plastic behavior was also observed in the non-compatible PC/PS system, the superplasticity clearly resulted from the constraint of the outer ductile film to the PS rather than the blending of these polymers.

References

1. I. M. WARD, "Mechanical Properties of Solid Polymers," 2nd ed. (John Wiley & Sons press, 1983).
2. R. P. KAMBOUR, *J. Polym. Sci. Macromol. Rev.* **7** (1973) 1.
3. S. RABINOWITZ and P. BEARDMORE, *CRC Reviews in Macromol. Sci.* **1** (1972) 1.
4. A. N. GENT, "The Mechanics of Fracture," *AMD* Vol. 19 (New, York, ASME 1976) p. 55.
5. A. M. DONALD and E. J. KRAMER, *Phil. Mag.* **A43** (1981) 857.
6. E. J. KRAMER, *Advances in Polymer Science* **52/53** (1983) 1.

7. H. H. KAUSCH, "Polymer Fracture" (Springer-Verlag, Heidelberg, 1978).
8. B. D. LAUTERWASSER and E. J. KRAMER, *Phil. Mag.* **A39** (1979) 469.
9. H. R. BROWN, *J. Mater. Sci.* **14** (1979) 237.
10. A. M. DONALD, E. J. KRAMER and R. A. BUBECK, *J. Polym. Sci.: Polym. Phys. Ed.* **20** (1982) 1129.
11. N. VERHUELPEN-HEYMANS, *Polymer* **20** (1979) 356.
12. J. S. TRENT, I. PALLEY and E. BAER, *J. Mater. Sci.* **16** (1981) 331.
13. A. C.-M. YANG, M. S. KUNZ and J. A. LOGAN, *Macromol.* **26** (1993) 1767.
14. R. E. ROBERTSON, *J. Appl. Polym. Sci.* **7** (1963) 443.
15. N. BROWN and I. M. WARD, *J. Polym. Sci. A-2* **6** (1968) 607.
16. I. M. WARD, *J. Mater. Sci.* **6** (1971) 1397.
17. B. L. GREGORY, A. SIEGMANN, J. IM, A. HILTNER and E. BAER, *J. Mater. Sci.* **22** (1987) 532.
18. S. J. PAN, J. IM, M. J. HILL, A. KELLER, A. HILTNER and E. BAER, *J. Polym. Sci.: Polym. Phys. Ed* **28** (1990) 1105.
19. M. MA, K. VIJAYAN, A. HILTNER, J. IM and E. BAER, *J. Mater. Sci.* **25** (1990) 2039.
20. E. SHIN, A. HILTNER and E. BAER, *J. Appl. Polym. Sci.* **47** (1993) 269.
21. D. HADERSKI, K. SUNG, J. IM, A. HILTNER and E. BAER, *ibid.* **52** (1994) 121.
22. K. SUNG, D. HADERSKI, A. HILTNER and E. BAER, *ibid.* **52** (1994) 147.
23. C. X. ZHU, S. UMEMOTO, N. OKUI and T. SAKAI, *J. Mater. Sci.* **23** (1988) 4091.
24. *Idem., ibid.* **24** (1989) 2787.
25. I. H. HAL, *J. Appl. Polym. Sci.* **12** (1968) 731.
26. M. WADA, T. NAKAMURA and N. KINOSHITA, *Phil. Mag.* **A38** (1978) 167.
27. A. C.-M, YANG and T. W. WU, *J. Mater. Sci.* **28** (1993) 955.
28. A. C.-M, YANG, R. C. WANG and J. H. LIN, *Polymer* **37** (1996) 5751.
29. G. D. MERFELD, A. DARIM, B. MAJUMDAR, S. K. SATIJA and D. R. PAUL, *J. Polym. Sci.: Polym. Phys. Ed* **36** (1998) 3115.
30. J. WASHIYAMA, E. J. KRAMER and C.-Y. HUI, *ibid.* **26** (1993) 2928.
31. A. M. DONALD and E. J. KRAMER, *Polymer* **23** (1982) 457.
32. A. M. DONALD, T. CHAN and E. J. KRAMER, *J. Mater. Sci.* **16** (1981) 669.
33. E. J. KRAMER, *Polym. Eng. & Sci.* **24** (1984) 761.
34. L. L. BERGER and E. J. KRAMER, *Macromol.* **20** (1987) 1980.
35. C. S. HENKEE and E. J. KRAMER, *J. Mat. Sci.* **21** (1986) 1398.
36. C. B. BUCKNALL, "Toughened Plastics" (Applied Science, London, 1977).
37. T. RICCO, A. PAVAN and F. DANUSSO, *Polym. Eng. & Sci.* **18** (1978) 774.
38. L. J. BROUTMAN and G. PANIZZA, *Int. J. Polym., Mater.* **1** (1971) 95.
39. C. H. LIN and A. C.-M. YANG, in preparation.
40. K. R. SHULL and E. J. KRAMER, *Macromol.* **23** (1990) 4780.
41. H. R. BROWN, *ibid.* **24** (1191) 2752.
42. KEVIN H. DAI, E. J. KRAMER and K. R. SHULL, *ibid.* **25** (1992) 220.
43. C. CRETON, E. J. KRAMER, C.-Y. HUI and H. R. BROWN, *ibid.* **25** (1992) 3075.

Received 12 November 1999
and accepted 13 January 2000